Acyl-CoA synthetase 1 deficiency alters cardiolipin species and impairs mitochondrial function

Trisha J. Grevengoed,* Sarah A. Martin,† Lalage Katunga,§ Daniel E. Cooper,* Ethan J. Anderson,§ Robert C. Murphy,† and Rosalind A. Coleman[1,*]

Department of Nutrition,* University of North Carolina at Chapel Hill, NC 27599; Department of Pharmacology,† University of Colorado, Anschutz Medical Campus, Aurora, CO 80045; and Department of Pharmacology and Toxicology,§ East Carolina University, Greenville, NC 27858

Abstract Long-chain acyl-CoA synthetase 1 (ACSL1) contributes more than 90% of total cardiac ACSL activity, but its role in phospholipid synthesis has not been determined. Mice with an inducible knockout of ACSL1 (*Acsl1*$^{T-/-}$) have impaired cardiac fatty acid oxidation and rely on glucose for ATP production. Because ACSL1 exhibited a strong substrate preference for linoleate, we investigated the composition of heart phospholipids. *Acsl1*$^{T-/-}$ hearts contained 83% less tetralinoleoyl-cardiolipin (CL), the major form present in control hearts. A stable knockdown of ACSL1 in H9c2 rat cardiomyocytes resulted in low incorporation of linoleate into CL and in diminished incorporation of palmitate and oleate into other phospholipids. Overexpression of ACSL1 in H9c2 and HEK-293 cells increased incorporation of linoleate into CL and other phospholipids. To determine whether increasing the content of linoleate in CL would improve mitochondrial respiratory function in *Acsl1*$^{T-/-}$ hearts, control and *Acsl1*$^{T-/-}$ mice were fed a high-linoleate diet; this diet normalized the amount of tetralinoleoyl-CL but did not improve respiratory function. Thus, ACSL1 is required for the normal composition of several phospholipid species in heart. Although ACSL1 determines the acyl-chain composition of heart CL, a high tetralinoleoyl-CL content may not be required for normal function.—Grevengoed, T. J., S. A. Martin, L. Katunga, D. E. Cooper, E. J. Anderson, R. C. Murphy, and R. A. Coleman. **Acyl-CoA synthetase 1 deficiency alters cardiolipin species and impairs mitochondrial function. *J. Lipid Res.* 2015.** 56: **1572–1582**.

Supplementary key words heart fatty acid/metabolism • fatty acid/oxidation • phospholipids/biosynthesis • phospholipids/metabolism • cardiomyocyte dysfunction

In order to metabolize long-chain fatty acids in pathways of β-oxidation or the synthesis of complex lipids, they must first be activated to acyl-CoAs by long-chain acyl-CoA synthetases (ACSLs). The five mammalian ACSL isoforms each have a specific substrate preference, subcellular location, and tissue distribution (1). In the heart, the ACSL1 isoform predominates, such that with deficiency, total ACSL specific activity and fatty acid oxidation decrease by more than 90% (2). Because ACSL activity is required for the incorporation of fatty acids into phospholipids, we asked whether the ACSL1 isoform is also required for the synthesis and remodeling of cardiac phospholipids, particularly cardiolipin (CL).

The mitochondrial phospholipid CL contributes to many aspects of mitochondrial function, including energy production through oxidative phosphorylation (3, 4), mitochondrial fission and fusion (5, 6), and cellular apoptosis (7). Tetralinoleoyl-CL is the predominant CL species in the mammalian heart (8), but the mechanism by which this species is formed is unclear. Because the enzymes of CL synthesis lack acyl-chain specificity, nascent CL contains a mixture of acyl chain lengths and degrees of unsaturation (9). To obtain mature CL, most remodeling occurs within the mitochondria by sequentially removing each acyl chain to form monolyso-CL (MLCL) and then replacing the missing fatty acid with linoleate (18:2). Linoleate is added by transacylation from a donor phospholipid (10) or by direct esterification of a linoleoyl-CoA (11, 12).

The transacylase tafazzin is believed to be responsible for cardiolipin remodeling. Mutations in tafazzin cause Barth syndrome, an X-linked cardiomyopathy characterized by skeletal muscle weakness and heart failure in

This work was supported by National Institutes of Health grants DK59935 (R.A.C.), U54-HL117798 (R.C.M.), HL122863 (E.J.A.), and F31-NS080486 (S.A.M.); by University of North Carolina Nutrition Obesity Research Center grant DK056350; by National Institutes of Health Predoctoral Training grant T32HL069768 (T.J.G.); and by American Heart Association Mid-Atlantic Division predoctoral fellowship grants 13PRE16910109 (T.J.G.) and 12GRNT12030144 (R.A.C.).

Manuscript received 31 March 2015 and in revised form 24 June 2015.

Published, JLR Papers in Press, July 1, 2015
DOI 10.1194/jlr.M059717

Abbreviations: ASM, acid soluble metabolite; ACSL, long-chain acyl-CoA synthetase; ACSL1, long-chain acyl-CoA synthetase 1; CL, cardiolipin; FCCP, 2-[[4-(trifluoromethoxy)phenyl]hydrazinylidene]propanedinitrile; MLCL, monolyso-cardiolipin; PC, phosphatidylcholine; PE, phosphatidylethanolamine; PI, phosphatidylinositol.

[1]To whom correspondence should be addressed.
e-mail: rcoleman@unc.edu

childhood (13). Hearts with tafazzin loss-of-function mutations contain low levels of tetralinoleoyl-CL and have a high ratio of MLCL to CL. Because tafazzin does not have a substrate preference for linoleate, it has been proposed that the linoleate enrichment of CL must be due to either an alteration in the physical shape of CL or by the action of an additional enzyme (10).

Here we show that ACSL1, which has a distinct preference for linoleate, significantly contributes to CL remodeling. Because fatty acids must be converted to acyl-CoAs to be available for the initial steps in the synthesis of phospholipids and to enter the mitochondrial matrix where CL remodeling occurs, we asked whether ACSL1 might be responsible for activating linoleate destined to be incorporated into CL. We found that hearts lacking ACSL1 are deficient in tetralinoleoyl-CL but that normalizing the CL species cannot ameliorate the mitochondrial dysfunction present in these hearts. These findings call into question the idea that the acyl-chains of CL are important for cardiac and mitochondrial respiratory function.

MATERIALS AND METHODS

Animal care and diets

All protocols were approved by the Institutional Animal Care and Use Committee at University of North Carolina at Chapel Hill. Mice were group housed under a 12 h light/dark cycle with free access to food and water. Unless otherwise specified, mice were fed a purified low-fat diet (Research Diets, DB12451B). A multitissue knockout of ACSL1 was achieved by mating mice with loxP sequences flanking exon 1 of the *Acsl1* gene to animals expressing a tamoxifen-inducible Cre driven by a ubiquitous promoter enhancer (2). Between 6 and 8 weeks of age, $Acsl1^{T-/-}$ and littermate control $Acsl1^{flox/flox}$ (control) mice were injected intraperitoneally on four consecutive days with 20 mg/ml (75 μg/g body weight) tamoxifen dissolved in corn oil. All studies were performed 20 weeks after tamoxifen was injected unless otherwise specified. Cardiac echocardiography was performed (blinded to mouse type) on conscious mice using a VisualSonics Vevo 770 or Vevo 2100 ultrasound biomicroscopy system (VisualSonics, Inc.). A model 707B (30 MHz) or model MS-550D (22–55 MHz) scan head was used on the Vevo 770 and Vevo 2100, respectively, as previously described (14). Two-dimensional guided M-mode echocardiography was performed in the parasternal long-axis view at the level of the papillary muscle on loosely restrained conscious mice. Wall thickness was then determined by measurements of epicardial to endocardial leading edges. For the diet study, group-housed mice were fed a high-linoleate safflower oil diet [Research Diets, D02062104, 45% kcal fat (75% linoleate)] for 4 weeks and were weighed weekly.

ACSL activity assay

ACSL specific activity was measured in heart membranes and cell homogenates (2). Briefly, homogenized tissues were centrifuged at 100,000 *g* for 1 h at 4°C to isolate total membrane fractions. Between 1 and 6 μg of protein was incubated with 50 μM [1-^{14}C]fatty acid (unless otherwise indicated), 10 mM ATP, 250 μM CoA, 5 mM dithiothreitol, and 8 mM $MgCl_2$ in 175 mM Tris (pH 7.4) at room temperature for 10 min. The enzyme reaction was stopped with 1 ml of Dole's solution (heptane-isopropanol-1 M H_2SO_4; 80:20:1; v/v). Two milliliters of heptane and 0.5 ml of water were added to separate phases. Radioactivity of the acyl-CoAs in the aqueous phase was measured using a liquid scintillation counter.

Mitochondrial function studies

Mitochondrial function was measured in permeabilized myofibers and in isolated mitochondria prepared from portions of the left ventricle and septum. After dissection, muscle samples were placed in ice-cold (4°C) Buffer X containing (in mM): 7.23 K_2EGTA, 2.77 CaK_2EGTA, 20 imidazole, 20 taurine, 5.7 ATP, 14.3 phosphocreatine, 6.56 $MgCl_2$-$6H_2O$, and 50 MES (pH 7.1, 295 mOsm). Fibers were delicately separated in ice-cold Buffer X using fine forceps under a dissecting scope. Cardiac fibers were then permeabilized in Buffer X with 50 μg/ml saponin for 30 min and then washed in ice-cold wash buffer Z (110 mM K-MES, 35 mM KCl, 1 mM EGTA, 5 mM K_2HPO_4, 3 mM $MgCl_2 \cdot 6H_2O$, 5 mg/ml BSA [pH 7.1, 295 mOsm]) to remove endogenous substrates. To prevent Ca^{2+} independent contraction of the permeabilized fibers, 20 μM blebbistatin was added to Buffer Z during wash and experiments. All mitochondrial O_2 consumption (JO_2) measurements were performed at 30°C using the Oroboros O_2K Oxygraph system (Oroboros Instruments). The H_2O_2 and Ca^{2+} uptake measurements were performed in a spectrofluorometer (Photon Technology Instruments or Horiba Jobin Yvon), equipped with a thermo-jacketed cuvette chamber. All mitochondrial experiments were performed in Buffer Z plus 5 mg/ml BSA. Consumption of O_2 was measured with either 5 mM pyruvate plus 2 mM malate or 125 μM palmitoyl-carnitine plus 2 mM malate. State 3 respiration was induced by adding ADP as indicated in the figure legends.

The rate of ATP production within the permeabilized myofibers was continuously recorded alongside the O_2 consumption in real time by monitoring the increasing fluorescence in the respiration chamber coming from NADPH (340ex/460em) with a spectrofluorometer as described (15). To maintain this reaction, 2.5 U/ml of glucose-6-phosphate dehydrogenase (Roche), 2.5 U/ml yeast hexokinase (Roche), 5 mM nicotinamide adenine dinucleotide phosphate ($NADP^+$) (Sigma-Aldrich), and 5 mM D-glucose (Sigma-Aldrich) were added to the assay media. P1,P5-Di(adenosine-5′)pentaphosphate (Ap5A) (Sigma-Aldrich) was included in the respiration medium to inhibit adenylate kinase and to ensure that ATP production was solely due to mitochondrial oxidative phosphorylation. An absolute amount of ATP generated across a given time frame was then calculated using a standard curve of fixed concentrations of ATP added to the saturating amounts of hexokinase, glucose, G6PDH, and $NADP^+$. Mitochondrial H_2O_2 emission was detected using Amplex UltraRed reagent (Invitrogen) in the presence of 1 U/ml HRP and 25 U/ml superoxide dismutase. The rate of H_2O_2 produced from the mitochondrial electron transport system supported by 125 μM palmitoyl-L-carnitine, 5 mM glutamate, and 5 mM succinate oxidation was determined in permeabilized fibers with 100 μM ADP, 5 mM glucose, and 1 U/ml hexokinase present to maintain the mitochondria in a permanent, submaximal phosphorylating state.

To isolate mitochondria, hearts were minced in 0.125 mg/ml trypsin in homogenization buffer (0.25 M sucrose, 10 mM HEPES, 1 mM EDTA [pH 7.4]). Soybean trypsin inhibitor (0.65 mg/ml) was added, and tissues were homogenized and centrifuged at 500 *g* for 5 min to remove nuclei and unbroken cells. Mitochondria were isolated by centrifuging at 10,000 *g* for 15 min and washed twice with homogenization buffer. Calcium uptake was measured in Buffer Z using 1 μM Calcium Green 5-N with 1 μM thapsigargin (Sigma-Aldrich) added to inhibit SERCA, a calcium transport ATPase. In separate experiments, the function of isolated mitochondria was assessed using a Seahorse

XF24 Analyzer. Mitochondria (15 μg protein) were stimulated sequentially with 100 μM ADP, 1.26 μM oligomycin, 4 μM 2-[[4-(trifluoromethoxy)phenyl]hydrazinylidene]propanedinitrile (FCCP), and 4 μm antimycin A (Sigma-Aldrich).

Phosphate quantification

Lipids were extracted from approximately 15 mg of ventricular myocardium, and phospholipids were separated by TLC on LK5D silica gel 150 Å plates (Whatman) in chloroform:ethanol:water:triethylamine (30:35:7:35; v/v) with authentic standards (16). Phosphate was quantified in the scraped silica regions for each phospholipid. The reaction was initiated by adding 30 μl 10% $Mg(NO_3)_2$ in ethanol to each sample and heating over an open flame (17). After adding 300 μl 0.5 N HCl, samples were boiled for 15 min. Then, 700 μl of a solution of 1.43% ascorbic acid and 0.36% ammonium molybdate in 0.86 N sulfuric acid was added, and the mixture was incubated at 45°C for 20 min. The absorbance of samples and a standard curve of sodium phosphate were measured at 605 nm.

Sample preparation for MS

Samples of left ventricle were homogenized on ice using a Dounce homogenizer in 50 mM phosphate buffer (pH 7.2), 0.1 M NaCl, 2 mM EDTA, 1 mM dithiothreitol, and protease inhibitors (Roche). Protein was determined by the bicinchoninic acid method (Pierce Biotechnology). Preparations of heart mitochondria (180 μg protein) or total left ventricle (300 μg protein) were diluted with 50 mM PBS to a total volume of 200 μl. An internal standard mixture was made in 100% methanol containing 1-dodecanoyl-2-tridecanoyl-*sn*-glycero-3-phosphate (PA-12:0/13:0), 1-dodecanoyl-2-tridecanoyl-*sn*-glycero-3-phosphocholine (PC-12:0/13:0), 1-dodecanoyl-2-tridecanoyl-*sn*-glycero-3-phosphoethanolamine (PE-12:0/13:0), 1-dodecanoyl-2-tridecanoyl-*sn*-glycero-3-phosphoglycerol (PG-12:0/13:0), 1-dodecanoyl-2-tridecanoyl-*sn*-glycero-3-phosphoinositol (PI-12:0/13:0), 1-dodecanoyl-2-tridecanoyl-*sn*-glycero-3-phosphoserine (PS-12:0/13:0), and 1′-[1,2-di-(9*Z*-tetradecenoyl)-*sn*-glycero-3-phospho], 3′-[1-(9*Z*-tetradecenoyl), 2-(10*Z*-pentadecenoyl)-*sn*-glycero-3-phospho]*sn*-glycero [CL- (14:1) x3/15:1]. Then 750 μl of methanol:chloroform (2:1; v/v) and an internal standard mixture (for mitochondrial preparations and left ventricles on low-fat diet, 50 ng of each phospholipid class and 100 ng of CL; for left ventricles on safflower oil diet, 25 ng of each phospholipid class and 100 ng of CL) was added, and products were extracted (18). The samples were dried under a stream of nitrogen and were then resuspended in 100 μl of 75% solvent A (isopropanol:hexanes; 4:3; v/v) and 25% solvent B (isopropanol:hexanes:water, 4:3:0.7 [v/v], containing 5 mM $C_2H_3O_2NH_4$). Samples were analyzed by LC/MS/MS as described below.

LC/MS

For normal phase separation, samples were injected onto an Ascentis-Si HPLC column (150 × 2.1 mm, 5 μm; Supelco) at a flow rate of 0.2 ml/min with 25% solvent B and 75% solvent A. Solvent B was maintained at 25% for 5 min, increased to 60% over 10 min, and then increased to 95% over 5 min. The system was held at 95% Solvent B for 20 min before re-equilibration at 25% for 14 min. Phospholipids were measured using an API3200 triple quadrupole mass spectrometer (AB Sciex). Positive ion mode was used to detect phosphatidylcholine (PC) and phosphatidylethanolamine (PE) lipids with quadrupole 1 scanning a *m/z* range from 250 to 1,100 in 0.1 Da increments over 2 s. Negative ion mode was used to detect CL, phosphatidic acid, phosphatidylinositol (PI), phosphatidylglycerol, and phosphatidylserine with quadrupole 1 scanning an *m/z* range from 150 to 1600 in 0.1 Da increments over 4 s. Quantitation was performed using AB Sciex MultiQuant software and using the internal standards for each phospholipid analyzed. Quantified data were corrected for isotope abundance. Fragmentation of endogenous lipids of *m/z* 818.5, 842.6, 844.6, 846.5, 864.5, and 890.5 (PC); 742.5, 738.5, 790.5, 762.5 (PE); 885.5 (PI); and 1448.0 (CL) was performed as described above, except for the following details. In the MS/MS experiment, the parent ions listed above were selected in quadrupole 1 and subjected to collision-induced decomposition using N_2 gas, and quadrupole 2 was allowed to scan the product ions in the *m/z* range from 150 to 900 (*m/z* 818.5, 842.6, 844.6, 846.5, 864.5, 890.5, 742.5, 738.5, 790.5, 762.5, and 885.5) or 150 to 1,450 (*m/z* 1448.0). After each of these specific phospholipid molecular species was identified, the number of acyl carbons and double bonds present in the set of fragment molecule was confirmed. From these data, the other phospholipids were converted from mass-to-charge to number of acyl carbons and double bonds.

Generation of stable ACSL1-knockdown H9c2 cells

Acsl1 rat shRNA or *scrambled* control shRNA constructs in pGFP-C-shLenti vector (Origene) were cotransfected with pHR-CMV-Δ8.2 and pCMB-VSV-G vectors in HEK293T cells to generate lentivirus. H9c2 cells (rat cardiomyocytes; ATCC) were incubated with media containing lentivirus for *Acsl1* shRNA or *scrambled* shRNA for 24 h. Cells were treated with 1 μM puromycin for 7 days to select cells that contained the shRNA. Knockdown of ACSL1 was confirmed by mRNA, protein, and ACSL enzyme activity.

Cellular phospholipid incorporation

H9c2 cells were cultured to confluence in 25 mM glucose DMEM with 10% FBS. Cells were differentiated for 4 days in 5 mM glucose DMEM with 1% horse serum. For overexpression experiments, cells were infected with adenovirus containing either *GFP* or *Acsl1-FLAG* (multiplicity of infection of 150) for 24 h. Cells were incubated with 0.5 μCi [1-^{14}C]palmitate, [1-^{14}C]oleate, or [1-^{14}C]linoleate for 6 h and then washed twice with 1% BSA. HEK-293 cells were grown to 50% confluence in 25 mM glucose DMEM with 10% FBS and then infected with adenovirus containing either *GFP* or *Acsl1-FLAG* (multiplicity of infection of 2.5) for 24 h. Cells were then incubated with a mixture of 30 μM oleate, 15 μM palmitate, and 5 μM linoleate plus 0.5 μCi of either [1-^{14}C]palmitate, [1-^{14}C]oleate, or [1-^{14}C]linoleate for an additional 24 h. For oxidation measurements, 0.4 ml media was collected in a tube containing 20 μL 15% BSA and then incubated with 100 μL 20% perchloric acid overnight at 4°C. The acidified media was centrifuged at 20,000 rpm for 5 min, and radioactivity in the supernatant was counted to determine acid-soluble metabolites (ASMs).

Microscopy

H9c2 cells grown on glass coverslips were incubated with 200 nM MitoTracker CMXRos (Life Technologies) for 30 min, fixed with 3.7% paraformaldehyde, and permeabilized with 0.2% Triton X-100. Cells were incubated with primary antibody [FLAG (Sigma) and/or Grp78 (Novus Biologicals)] for 2 h and then secondary antibody (Alexafluor 488 or 568; Life Technologies) for 1 h. Cells were then incubated with DAPI (Life Technologies) for 5 min, mounted on glass slides with Prolong Gold (Life Technologies), and visualized with a Zeiss 710 confocal microscope.

Statistics

Data are presented as the mean ± SE for each group. Differences between genotypes were evaluated by Student's *t*-test. For

experiments with multiple treatments or diets, differences between groups were evaluated by two-way ANOVA with Tukey multiple-comparison post-tests. Differences between means with $P < 0.05$ were considered statistically significant.

RESULTS

ACSL1 was located on cardiac mitochondria and preferred to activate linoleate

Cardiac ACSL1 protein and ACSL specific activity were enriched in the mitochondrial fraction compared with whole tissue (**Fig. 1A**, B). Purified recombinant ACSL1 from rat liver shows a broad fatty acid substrate preference with varying chain lengths and degrees of unsaturation (19). To determine the fatty acid substrate preference in mouse heart, long-chain acyl-CoA synthetase (ACSL) activity was assayed with different fatty acid substrates in total membrane preparations from control and *Acsl1*$^{T-/-}$ hearts. Control hearts exhibited the highest ACSL activity with linoleate (18:2) (Fig. 1C). This clear substrate preference was lost in *Acsl1*$^{T-/-}$ hearts, which lack more than 90% of total ACSL activity with all fatty acids (Fig. 1D), indicating that the preferential activation of linoleate was due to ACSL1 activity.

Loss of ACSL1 caused mitochondrial dysfunction

Acsl1$^{T-/-}$ and littermate control mice were injected with tamoxifen at 6–8 weeks to produce ACSL1 deficiency. Ten weeks after tamoxifen injection, *Acsl1*$^{T-/-}$ hearts are enlarged but have normal systolic function (2). To determine whether function worsens with time, echocardiography was performed 20 weeks after initiating the ACSL1 knockout. *Acsl1*$^{T-/-}$ hearts remained hypertrophied, with no impairment in contractile function (**Fig. 2**A–C). To determine whether loss of ACSL1 caused mitochondrial dysfunction, O_2 consumption in saponin-permeabilized cardiac muscle fibers was measured using palmitoyl-carnitine and malate (Fig. 2D) or pyruvate and malate (Fig. 2E) with increasing concentrations of ADP or succinate. Basal O_2 consumption rate was normal in *Acsl1*$^{T-/-}$ mitochondria, but, compared with controls, the mitochondrial response to ADP stimulation was 56% lower. In addition to impaired ADP-stimulated oxygen consumption, *Acsl1*$^{T-/-}$ mitochondria produced less ATP for each O_2 molecule consumed, indicative of inefficient energy production (Fig. 2F). Although many models of mitochondrial dysfunction produce increased amounts of H_2O_2, *Acsl1*$^{T-/-}$ mitochondria did not, possibly due to their lower metabolic rate (Fig. 2G). Isolated *Acsl1*$^{T-/-}$ mitochondria took up less calcium than controls before reaching the permeability transition (Fig. 2H), suggesting that *Acsl1*$^{T-/-}$ mitochondria may be more susceptible to stress and apoptosis. Calcium uptake into mitochondria increases oxygen consumption and NADH production, but once calcium uptake exceeds the permeability transition, mitochondria are more likely to become disrupted, release cytochrome c into the cytosol, and undergo apoptosis (20). Despite this severely impaired respiratory function, *Acsl1*$^{T-/-}$ mice do not develop heart failure under unstressed conditions (2) and have a normal lifespan (data not shown).

Loss of ACSL1 altered the acyl-chain composition of mitochondrial cardiolipin and phospholipids

Cardiolipin associates closely with complexes of the electron transport chain and is highly important for mitochondrial function (3, 4). Cardiac cardiolipin normally contains as much as 77% linoleate (8). Because ACSL1 has a distinct preference for linoleate, we questioned whether the loss of ACSL1 would affect the composition of cardiolipin and other phospholipids in cardiac mitochondria. The content of individual phospholipid species in cardiac ventricles did not differ between genotypes (**Fig. 3A**); however, in the knockout mice the average chain length and number of double bonds was lower (Fig. 3B, C). MS analysis revealed that loss of ACSL1 caused large changes in the

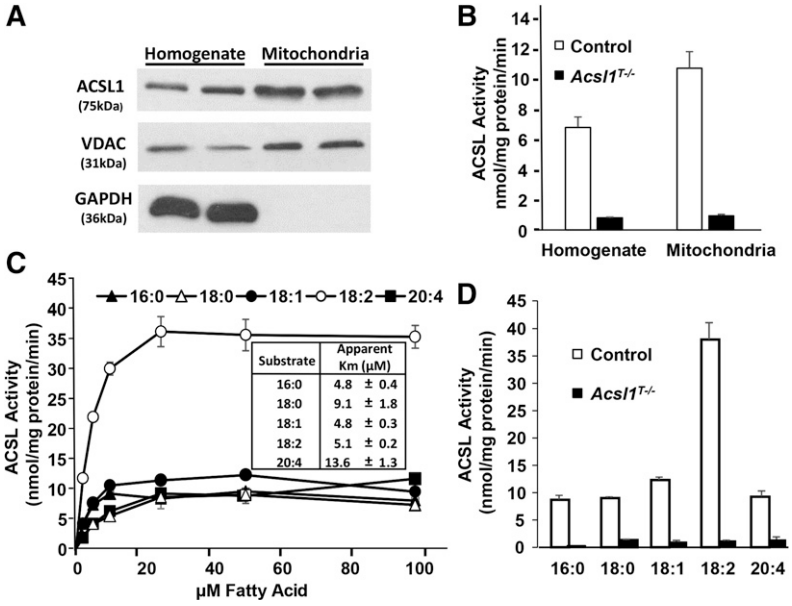

Fig. 1. ACSL1 is located on cardiac mitochondria and activates linoleate preferentially. A: ACSL1 protein from control heart homogenates and isolated mitochondria. B: ACSL activity of heart homogenates and mitochondria measured with 50 μM palmitate (n = 3). C: ACSL activity in total membrane fractions from control hearts measured with 2 μg protein and varying amounts of [^{14}C]labeled fatty acids (n = 3). D: ACSL activity in total membrane fractions from control and *Acsl1*$^{T-/-}$ mouse hearts measured with 2 μg protein and 50 μM of [^{14}C]labeled fatty acids (n = 3). * $P \leq 0.05$ between control and *Acsl1*$^{T-/-}$. VDAC, voltage-dependent anion channel.

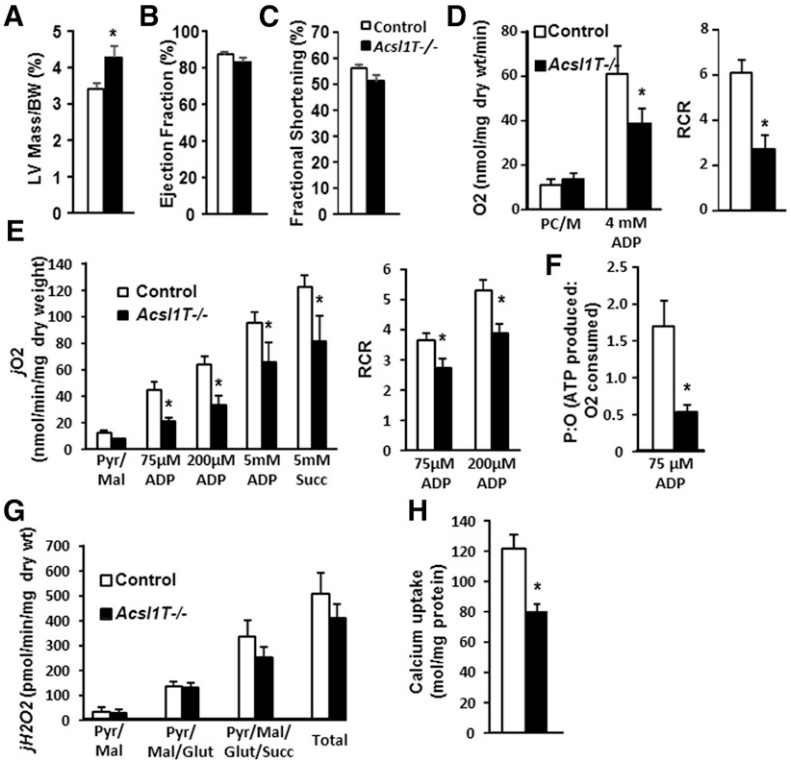

Fig. 2. Loss of ACSL1 caused mitochondrial dysfunction. A: Left ventricle (LV) mass normalized to body weight (n = 4). Ejection fraction (B) and fractional shortening (C) as measured by echocardiography on conscious mice (n = 4). Consumption of O_2 was measured in saponin-permeabilized cardiac muscle fibers with either (D) palmitoyl-carnitine + malate (PC/M) or (E) pyruvate + malate (Pyr/Mal) ± ADP and succinate (succ). RCR, respiratory control ratio. F: ratio of ADP-stimulated O_2 consumption to basal (n = 4–6). G: Ratio of ATP produced for each O_2 molecule consumed (n = 4–5). E: Hydrogen peroxide (H_2O_2) production (n = 6). H: Calcium uptake in isolated cardiac mitochondria before the permeability transition (n = 3). * $P \leq 0.05$ between control and *Acsl1*$^{T-/-}$.

acyl-chain composition of the major phospholipid species. As has been reported previously (8), the major cardiolipin (CL) species in control mouse hearts contained four linoleate acyl-chains (tetralinoleoyl-CL; 72:8-CL) (Fig. 3D). In the *Acsl1*$^{T-/-}$ mitochondria, however, this species was 83% lower, and compared with controls, the CL species containing two linoleate and two arachidonate acyl chains (76:12-CL) was 80% lower. *Acsl1*$^{T-/-}$ heart mitochondria contained larger amounts of CL species esterified with stearate (18:0) and oleate (18:1), indicating either that CL remodeling was impaired or that the availability of linoleate was limited.

To determine whether the loss of ACSL1 impaired linoleate incorporation into other phospholipids, several species were fragmented to identify the acyl chains present. Linoleate-containing species of PC and PE (36:3-PC, 36:2-PC, and 36:2-PE) were approximately 2- to 4-fold higher in *Acsl1*$^{T-/-}$ hearts than in controls. Excess linoleate in these species suggests that the absence of ACSL1, which is primarily located on the mitochondrial outer membrane, altered the incorporation of linoleoyl-CoA into PC and PE, which are synthesized and remodeled on the endoplasmic reticulum. Furthermore, the excess linoleate present in mitochondrial PC and PE was consistent with impaired transacylation from these donor phospholipids. Compared with controls, the expression of the transacylase tafazzin was 31% lower in *Acsl1*$^{T-/-}$ hearts (Fig. 3H), suggesting an explanation for both excess linoleate in PC and PE and the diminished tetralinoleoyl-CL, although we did not observe the increase in MLCL that is a hallmark of tafazzin deficiency.

Loss of ACSL1 altered other mitochondrial phosphatidylinositol (PI), PC, and PE species (Fig. 3E–G), but no differences were seen in phosphatidylglycerol or phosphatidylserine (data not shown). In control mitochondria, the most abundant mitochondrial PI was 18:0, 20:4-PI. This species was 64% lower in the *Acsl1*$^{T-/-}$ hearts and was compensated for by a higher content of multiple minor PI species, so that the total content of PI was unchanged in the two genotypes. For PC, the major species in control hearts contained DHA (22:6) together with either palmitate (38:6-PC) or stearate (40:6-PC). Compared with controls, these species were 53% and 48% lower, respectively, in *Acsl1*$^{T-/-}$ hearts. PC species that contained DHA were replaced with oleate in the *Acsl1*$^{T-/-}$ mitochondria so that 16:0-18:1-PC (34:1-PC) was 2-fold higher and 18:0-18:1-PC (36:1-PC) was 3-fold higher than in control hearts. The major PE species in control hearts also contained DHA and stearate (40:6-PE) and was approximately 30% lower in the *Acsl1*$^{T-/-}$ hearts. Impaired activation of α-linolenate due to loss of ACSL1 at the peroxisomal membrane may result in decreased uptake into peroxisomes where DHA synthesis occurs (21). The compositions of PC and PE in isolated mitochondria from control and *Acsl1*$^{T-/-}$ ventricles were similar to those in total membranes (data not shown), supporting the idea that ACSL1 strongly influences phospholipid synthesis in the endoplasmic reticulum where these phospholipids are synthesized and remodeled (22).

Knockdown of *Acsl1* in H9c2 cardiomyocytes impaired the oxidation of fatty acid and its incorporation into complex lipids

To further investigate how the loss of ACSL1 affects phospholipid formation, we made a stable knockdown of *Acsl1* in H9c2 cells, a rat cardiomyocyte cell line. The

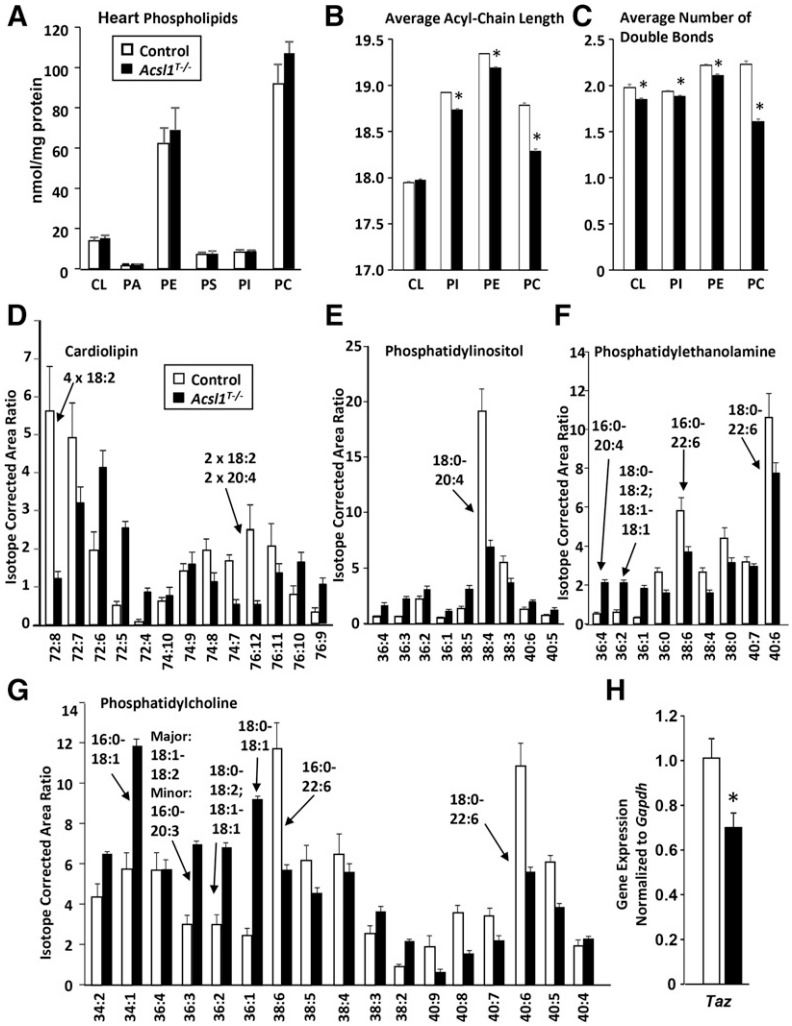

Fig. 3. Loss of ACSL1 alters acyl-chain composition of mitochondrial phospholipids. A: Quantification of phosphate in ventricular phospholipids separated by TLC (n = 5). B and C: Average acyl chain length (B) and double bonds in mitochondrial phospholipids (C) were calculated using the isotope corrected area ratio determined by LC/MS/MS (n = 5). D–F: LC/MS/MS analysis of phospholipid species in isolated mitochondria (n = 5). Phospholipid species are shown as relative amounts normalized to an internal standard for each phospholipid. Species that were fragmented are indicated with arrows and identified acyl chains. Other species were detected but were omitted from graph if the isotope corrected ratio was <2 and no difference between genotypes was found. G: Ventricular tafazzin gene expression (n = 4). * $P \leq 0.05$ between control and $Acsl1^{T-/-}$.

knockdown caused a 67% loss of *Acsl1* mRNA, a 55% reduction of ACSL1 protein, and a 26% decrease in total ACSL activity (**Fig. 4**A–C). To avoid high concentrations of fatty acid, which drives triacylglycerol synthesis, cells were incubated with trace amounts of individual [1-^{14}C] fatty acids (palmitate, oleate, or linoleate) to measure their incorporation into phospholipids. As measured by ASMs in the media, the oxidation of these fatty acids was 80% lower in the *Acsl1* knockdown cells than in controls (Fig. 4D), consistent with the requirement for ACSL1 in channeling long-chain fatty acids into the pathway of β-oxidation (2). Decreased ACSL1 also caused approximately 40% lower incorporation of fatty acids into total glycerolipids (Fig. 4E).

The ACSL1 knockdown in H9c2 cells greatly diminished incorporation of fatty acids into neutral lipids and PC (Fig. 4F, H). The incorporation of linoleate into CL was 32% lower in *Acsl1* knockdown cells (Fig. 4G), which is consistent with the low content of tetralinoleoyl-CL in the $Acsl1^{T-/-}$ hearts. Compared with control cells, the incorporation of palmitate into PC, PE, PS, and CL was lower by 43, 34, 17, and 46%, respectively (Fig. 4H). Consistent with $Acsl1^{T-/-}$ hearts, knockdown of ACSL1 resulted in a 57% loss of tafazzin mRNA (data not shown). In contrast to highly oxidative cardiomyocytes in vivo, cultured cells rely minimally on fatty acid oxidation for energy. Thus, compared with heart, in which palmitate is more readily oxidized, cultured cells activate more palmitate destined for esterification into phospholipids. Other than PC, in which 37% less oleate was incorporated, no differences in the incorporation of oleate into phospholipids were observed between control and *Acsl1* knockdown cells. Thus, in cultured cardiomyocytes, as in liver (23), loss of ACSL1 impaired the activation of fatty acids that were incorporated into TAG and phospholipids, with the largest effects found with palmitate and linoleate.

Overexpressed ACSL1 increased linoleate metabolism

To confirm the dependence of CL remodeling on linoleate that had been activated by ACSL1, ACSL1 was overexpressed in H9c2 cardiomyocytes (**Fig. 5A**), where it localized primarily to mitochondria (Fig. 5B). The *Ad-Acsl1* infection increased ACSL specific activity 3.3-fold (Fig. 5C). After a 6 h incubation with trace amounts of each of the [1-^{14}C]fatty acids, the cells overexpressing ACSL1 increased linoleate oxidation by 28%; however, the oxidation of palmitate and oleate did not change (Fig. 5D). ACSL1 overexpression increased palmitate and linoleate incorporation into total lipids by 17% and 26%, respectively (Fig. 5E). ACSL1 overexpression increased

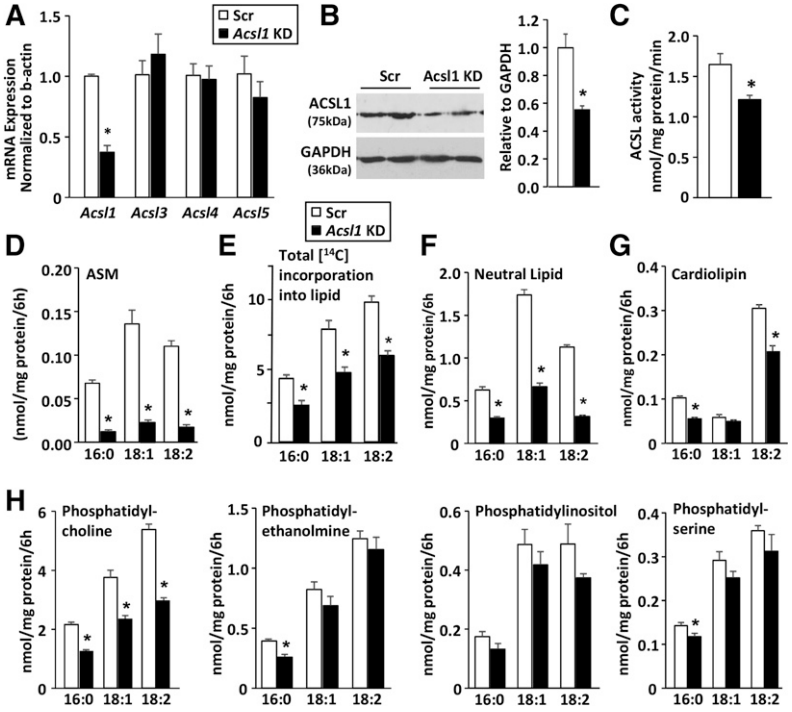

Fig. 4. Knockdown of ACSL1 impairs fatty acid oxidation and incorporation into lipids. H9c2 cells were infected with lentivirus to stably express shRNA for either *scrambled* control (*Scr*) or *Acsl1* knockdown (KD). A: mRNA abundance of *Acsl* isoforms (*Acsl6* was not detected). B: ACSL1 protein. C: ACSL activity measured with 50 μM palmitate. D: Cells were incubated with trace [1-^{14}C]fatty acid (0.5 μCi) for 6 h. Fatty acid oxidation was measured as ASM, a measure of incomplete fatty acid oxidation, in the media. E: Radioactivity in total cellular lipid extract. F–H: Lipids were separated by TLC, and radioactivity was quantified (n = 3 independent experiments, each performed in triplicate). * $P \leq 0.05$ between *Scr* and *Acsl1* KD.

linoleate incorporation into neutral lipid by 48%, cardiolipin by 28%, PC by 28%, and phosphatidylserine by 22% (Fig. 5F–H). Palmitate incorporation was less influenced by overexpressed ACSL1; its incorporation into PC, PI, and phosphatidylserine increased 17–18%, similar to the 17% increase seen in total lipid incorporation (Fig. 5F). In contrast to the association of low ACSL1 with diminished *tafazzin* abundance, ACSL1 overexpression did not raise *tafazzin* expression (data not shown). In heart and skeletal muscle, which both contain high proportions of tetralinoleoyl-CL (2, 23), the predominance of the ACSL1 isoform may underlie the enrichment in tetralinoleoyl-CL.

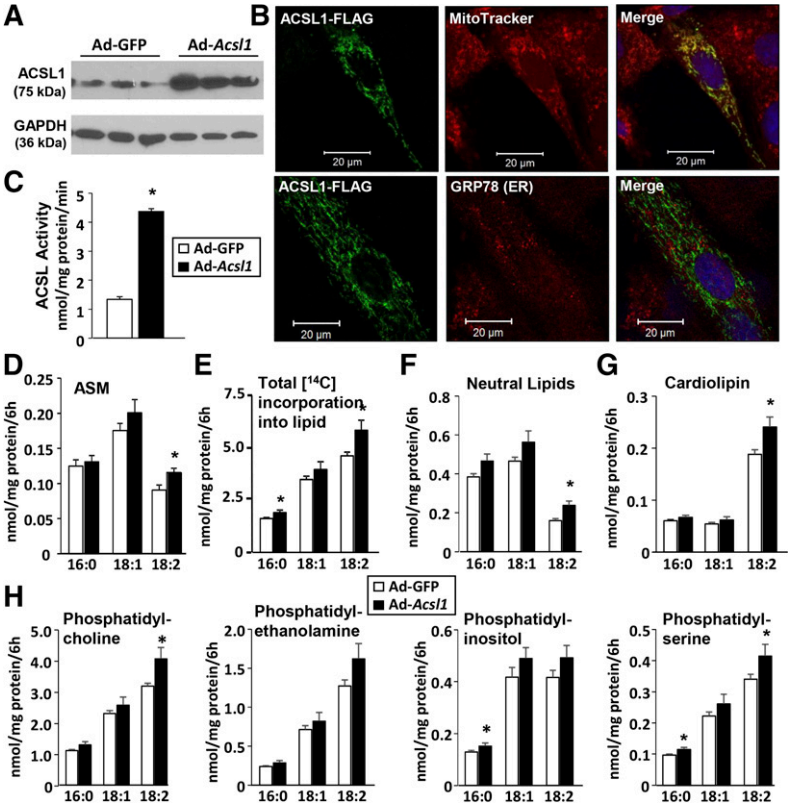

Fig. 5. Overexpression of ACSL1 increases linoleate metabolism. H9c2 cells were infected with either *Ad-GFP* or *Ad-Acsl1-FLAG*. A: ACSL1 protein. B: Subcellular localization of ACSL1-FLAG. C: ACSL activity measured using 50 μM [1-^{14}C]palmitate. D: After a 6 h incubation with trace amounts of [1-^{14}C]fatty acid (0.5 μCi), fatty acid oxidation was measured in ASMs (incomplete fatty acid oxidation) in the media. E: Radioactivity in total lipid extract. F–H: Lipids were separated by TLC, and radioactivity in each species was quantified (n = 3 independent experiments, each performed in triplicate). * $P \leq 0.05$ between *Ad-GFP* and *Ad-ACSL1-FLAG*.

ACSL1 overexpression increased linoleate incorporation into CL in HEK-293 cells

To determine whether the ability of ACSL1 to increase linoleate incorporation into CL was specific to cardiomyocytes, we overexpressed ACSL1 in HEK-293 cells, which normally contain little tetralinoleoyl-CL (24). Twenty-four hours after the *Ad-Acsl1* infection, ACSL1 protein was present, and total ACSL specific activity had increased 9-fold (**Fig. 6A**, B). At this time, cells were incubated for an additional 24 h with a mixture of fatty acids to mimic the percentages in a physiological mixture of monounsaturated, saturated, and polyunsaturated fatty acids (30 μM oleate, 15 μM palmitate, and 5 μM linoleate plus the addition of 0.5 μCi of either [1-^{14}C]labeled oleate, palmitate, or linoleate). ACSL1 overexpression increased palmitate incorporation into total lipids by 43%, oleate incorporation by 49%, and linoleate incorporation by 75% (Fig. 6C). The *Ad-Acsl1* infection did not alter the esterification of these fatty acids into neutral lipids (Fig. 6D), showing that the differences in total lipid incorporation were due to integration into phospholipids. ACSL1 overexpression resulted in 41% and 94% higher incorporation of palmitate and linoleate, respectively, into CL, but no difference was observed in oleate incorporation (Fig. 6E). ACSL1 increased the incorporation of each of the fatty acids into PC, PE, and PI/PS (Fig. 6F), phospholipids that are synthesized at the endoplasmic reticulum. The high incorporation of labeled fatty acids into these phospholipids is likely due to increased fatty acid uptake and elevated acyl-CoA concentrations in the cytosol, but, importantly, ACSL1 specifically increased linoleate incorporation into CL, which is remodeled within mitochondria. Enhanced linoleate retention in CL indicates that the synthesis of linoleoyl-CoA is sufficient for its preferential incorporation into CL, even in noncardiomyocytes.

Dietary linoleate enrichment normalized tetralinoleoyl-CL content but did not improve mitochondrial function in *Acsl1*$^{T-/-}$ hearts

The relevance of CL acyl-chain composition to normal oxidative phosphorylation is controversial (25, 26). In order to determine whether the impaired respiratory function of mitochondria from *Acsl1*$^{T-/-}$ hearts resulted from the presence of linoleate-deficient mitochondrial CL, we fed control and *Acsl1*$^{T-/-}$ mice a high safflower oil diet, in which 75% of the fatty acids are linoleate. Safflower oil feeding normalizes CL species in spontaneous hypertensive rats and improves their mitochondrial function (27). After 4 weeks, weights were lower for the *Acsl1*$^{T-/-}$ mice fed the safflower oil diet (*Acsl1*$^{T-/-}$, 27 g vs. controls, 35 g). The 4 weeks of safflower oil feeding markedly increased the total amount of linoleate in CL in both control and *Acsl1*$^{T-/-}$ hearts, although the abnormal ratio between control and *Acsl1*$^{T-/-}$ CL persisted, perhaps because the low linoleate activation resulted in lower cardiac uptake of this fatty acid species. The diet increased the amount of the tetralinoleoyl-CL species in *Acsl1*$^{T-/-}$ hearts 4-fold, compared with the amount present when the mice ate a low-fat diet. Importantly, the safflower oil diet increased the tetralinoleoyl-CL content of *Acsl1*$^{T-/-}$ hearts to a level

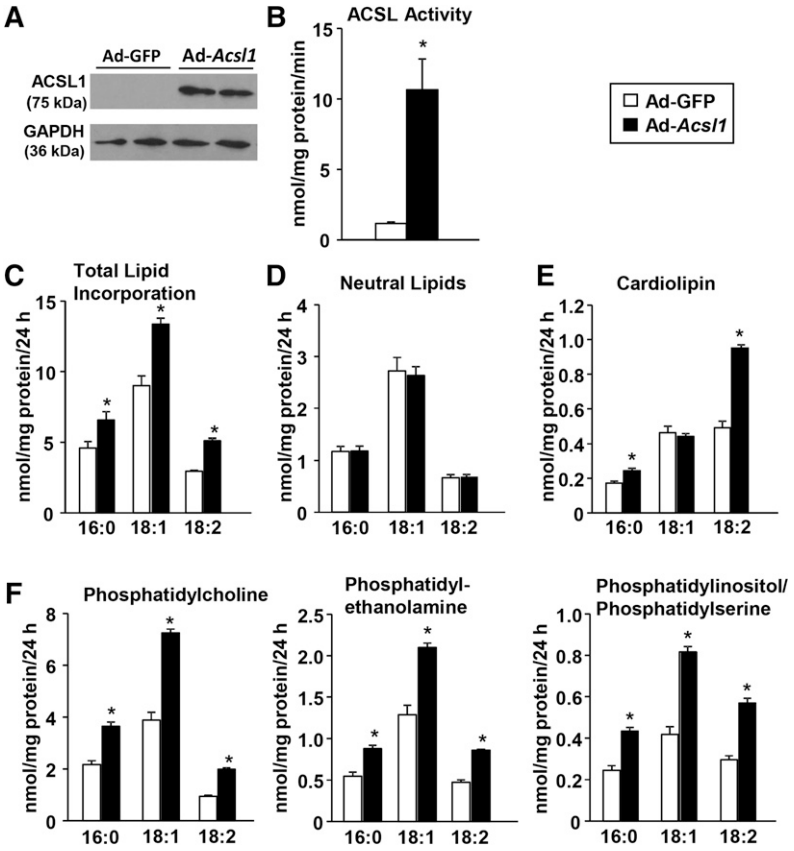

Fig. 6. ACSL1 overexpression increased linoleate incorporation into CL in HEK-293 cells. HEK-293 cells were infected with either *Ad-GFP* or *Ad-Acsl1-FLAG*. A: ACSL1 protein. B: ACSL specific activity measured with 50 μM [1-^{14}C]palmitate. C–F: Cells were incubated with 30 μM oleate, 15 μM palmitate, and 5 μM linoleate with 0.5 μCi [1-^{14}C]oleate, [1-^{14}C] palmitate, or [1-^{14}C]linoleate for 24 h. C: Radioactivity in total lipid extract. D–F: Lipids were separated by TLC, and radioactivity was quantified (n = 3 independent experiments, each performed in triplicate). * $P \leq 0.05$ between *Ad-GFP* and *Ad-ACSL1-FLAG*.

that was equal to the content in hearts from control mice fed the low-fat diet (**Fig. 7A**). *Tafazzin* expression was not altered by diet, and the normalization of tetralinoleoyl-CL content was not due to increased *tafazzin* expression, because the expression of this gene remained 25% lower in the safflower oil-fed $Acsl1^{T-/-}$ mice compared with controls (Fig. 7B). To determine the effect of normalized tetralinoleoyl-CL content on mitochondrial respiration, we measured the function of the electron transport chain in isolated mitochondria. Basal O_2 consumption did not differ between groups (Fig. 7C). Similar to the data from permeabilized cardiac fibers, $Acsl1^{T-/-}$ hearts contained functionally defective mitochondria, as shown by impaired responses to ADP and FCCP (Fig. 7D). In control mitochondria, safflower feeding increased respiration after oligomycin treatment but did not change the response to ADP or FCCP. However, despite the normalization of tetralinoleoyl-CL content, safflower oil feeding did not improve the respiratory function of mitochondria from $Acsl1^{T-/-}$ hearts, and responses to both ADP and the mitochondrial uncoupler FCCP remained 30–44% lower than controls (Fig. 7D).

DISCUSSION

CL is synthesized and remodeled within the mitochondria, but its precursors, phosphatidic acid and CDP-diacylglycerol, are formed primarily on the endoplasmic reticulum and are imported into the mitochondria where phosphatidylglycerol is synthesized (28). CL synthase then combines phosphatidylglycerol with the phosphatidyl group from a second molecule of CDP-diacylglycerol. Because CL synthase lacks a preference for phosphatidylglycerol or CDP-diacylglycerol species that contain linoleate (9, 29), the acyl-chains of the nascent CL are more highly saturated than those of mature cardiac CL. CL is remodeled by successive removal of acyl-chains by a phospholipase, followed by replacement of the acyl chain via tafazzin-mediated transacylation from donor phospholipids or by an acyltransferase-mediated esterification, which requires an acyl-CoA (10).

Although cardiac CL is highly remodeled after synthesis, the functional significance of the remodeling remains unknown. In *Saccharomyces cerevisiae* lacking tafazzin, an additional deletion of the CL-specific phospholipase, Cld1, prevents the accumulation of MLCL, inhibits CL remodeling, and rescues the mitochondrial respiratory defect, strongly suggesting that the respiratory defect had been due to the accumulation of MLCL and/or the decrease in the total content of CL (25). In mammalian cells, two additional enzymes, lysocardiolipin acyltransferase 1 (ALCAT1) and MLCL acyltransferase 1 (MLCL AT-1), can use acyl-CoAs to esterify MLCL (28). ALCAT1, however, is located on the ER, which would prevent its interaction with most CL (30), but MLCL AT-1 is present in mitochondria (11). Although overexpressing MLCL AT-1 in tafazzin-deficient lymphoblasts increases both linoleate incorporation into CL and total CL content (11), the importance of MLCL AT-1 for normal CL remodeling in heart cells remains unclear.

With its preference for linoleate, ACSL1 appears to be critical in maintaining the abundance of the tetralinoleoyl-CL species in the heart. This might occur in two ways: ACSL1-derived linoleoyl-CoA could be incorporated into donor phospholipids and then transacylated into CL, or the linoleoyl-CoA could be directly incorporated into MLCL by an acyltransferase. The mitochondria-located ACSL1 could increase the concentration of linoleoyl-CoA that is imported into mitochondria for β-oxidation or CL remodeling. Alternatively, because ACSL1 overexpression increases linoleate incorporation into PC, PE, and phosphatidylserine, its enhancement of CL species that contain linoleate could occur via transacylation of linoleate from

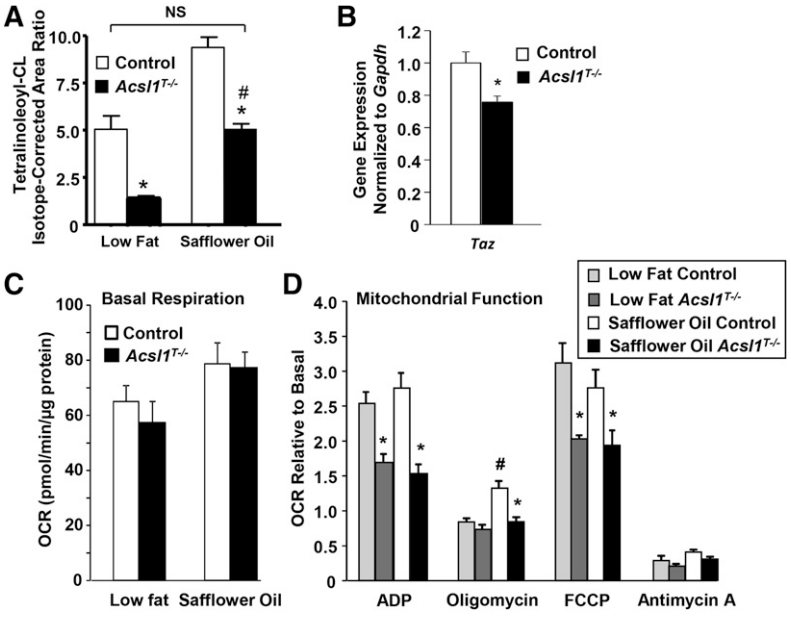

Fig. 7. High linoleate diet partially normalized CL acyl-chain profile in $Acsl1^{T-/-}$ hearts but did not improve mitochondrial respiratory function. For 16 weeks after tamoxifen injections, male mice were fed a low-fat (10% fat) control diet. Mice were then either maintained on the low-fat diet or switched to a high safflower oil diet (Research Diets, D02062104, 45% kcal fat; 75% linoleate) for 4 additional weeks to increase dietary linoleate. A: LC/MS/MS analysis of ventricular cardiolipin with low-fat and safflower oil diets (n = 5). B: Ventricular tafazzin gene expression in mice fed safflower oil (n = 5). C and D: Mitochondrial respiratory function was measured in isolated mitochondria using a Seahorse XF24 Analyzer, which sequentially injected ADP, oligomycin, FCCP, and antimycin A (n = 4–7). OCR, O_2 consumption rate. * $P \leq 0.05$ between genotypes within diet. # $P \leq 0.05$ between diets within genotype.

these phospholipids to CL or MLCL. However, if ACSL1 provides linoleoyl-CoA for phospholipid synthesis, it is surprising that the linoleate content of PC and PE was also greater in the absence of ACSL1. A likely explanation is that when ACSL1 is absent, linoleate increases within the cell and becomes available for activation by other ACSL isoforms that are present on the endoplasmic reticulum where the excess linoleoyl-CoA would be used during the synthesis of PC and PE. Because *tafazzin* mRNA was reduced in *Acsl1*$^{T-/-}$ hearts fed both control and high safflower oil diets and in ACSL1-deficient H9c2 cells, transacylation may also be impaired when ACSL1 is absent, thereby resulting in a diminished content of tetralinoleoyl-CL despite an abundance of linoleate in donor phospholipids. The substrate preference of mitochondria-located ACSL1 for linoleate would therefore be important for both the transacylase and the acyltransferase pathways of CL remodeling.

Diminished *tafazzin* expression in the context of lowered ACSL1 activity remains unexplained. In the heart-specific knockout of *Acsl1*, remarkable alterations were observed in the expression of genes related to activated mTORC1, but we did not identify *tafazzin* expression as being significantly reduced (31). The regulation of tafazzin has not been fully studied; however, decreased mRNA expression has been reported with thyroxine treatment (32), which results in an increase in total CL content without favoring the formation of tetralinoleoyl-CL (33). Heart failure also diminishes *tafazzin* expression (34) and tetralinoleoyl-CL content (35), demonstrating a physiological relationship between *tafazzin* expression and CL species. However, neither hyperthyroidism nor heart failure was present in the *Acsl1*$^{T-/-}$ mice.

Because the composition of the major CL species varies in different tissues, it is highly likely that the species formed depends on the fatty acid preference of the ACSL isoforms present. The substrate preferences originally reported for ACSL1 were investigated with recombinant rat ACSL1 protein purified from bacteria (36). The differences in substrate preference observed in our study may reflect the presence of cell membranes as well as mammalian posttranslational modifications by phosphorylation and acetylation (37), but additional studies must be performed to confirm this interpretation. The ER-localized ACSL isoforms would dictate which acyl-CoAs are incorporated into PC and PE, and the ACSL isoforms present on the outer mitochondrial membrane may synthesize acyl-CoAs that can be incorporated directly into CL. For instance, ACSL1 accounts for more than 90% of ACSL activity in both heart (2) and skeletal muscle (38) in which more than 75% of CL is tetralinoleoyl-CL (8). In contrast, tetralinoleoyl-CL is ~50% of the total CL species in liver (8), a tissue in which ACSL1 is responsible for only about 50% of total ACSL activity (23). Similarly, ACSL1 is minimally expressed in brain (39), in which the major CL acyl-chains are oleate and arachidonate (40). An analysis of the fatty acid preferences of other ACSL isoforms may explain tissue differences in CL composition.

In contrast to tafazzin-deficient mice, *Acsl1*$^{T-/-}$ hearts do not contain a low total CL content or excess MLCL. Thus, the *Acsl1*$^{T-/-}$ model allowed us to study CL remodeling in the presence of a normal CL content as well as the impact of impaired tetralinoleoyl-CL formation on heart and mitochondrial function. In *Acsl1*$^{T-/-}$ hearts, normalizing the amount of linoleate present in CL did not improve respiratory dysfunction. Similarly, in *S. cerevisiae*, CL remodeling can be inhibited without impairing basal or ADP-stimulated mitochondrial O_2 consumption (25, 26). Thus, in both yeast and in *Acsl1*$^{T-/-}$ hearts, when total CL content is normal, mitochondrial function appears to be independent of the presence of a specific CL species. In contrast, hearts from tafazzin-deficient mice and from people with Barth's syndrome contain both an increased content of MLCL and a reduction in total CL (8, 41, 42). These CL changes are associated with a dilated cardiomyopathy, cardiac respiratory dysfunction, and heart failure (43). Despite the presence of mitochondrial dysfunction, *Acsl1*$^{T-/-}$ mice do not develop heart failure, suggesting that when total CL abundance is normal, the absence of a high content of tetralinoleoyl-CL is not physiologically harmful. It will be important to determine whether the *Acsl1*$^{T-/-}$ hearts are more susceptible to impaired function when subjected to pressure overload. Conversely, normalizing tetralinoleoyl-CL in *Acsl1*$^{T-/-}$ hearts was not sufficient to improve mitochondrial respiratory function. Our data, together with the published yeast studies (25, 26), suggest that the underlying difficulty in Barth syndrome and tafazzin-deficient mice is a deficiency in CL content and/or the accumulation of MLCL.

REFERENCES

1. Coleman, R. A., T. M. Lewin, C. G. Van Horn, and M. R. Gonzalez-Baro. 2002. Do long-chain acyl-CoA synthetases regulate fatty acid entry into synthetic versus degradative pathways? *J. Nutr.* **132:** 2123–2126.
2. Ellis, J. M., S. M. Mentock, M. A. Depetrillo, T. R. Koves, S. Sen, S. M. Watkins, D. M. Muoio, G. W. Cline, H. Taegtmeyer, G. I. Shulman, et al. 2011. Mouse cardiac acyl coenzyme a synthetase 1 deficiency impairs fatty acid oxidation and induces cardiac hypertrophy. *Mol. Cell. Biol.* **31:** 1252–1262.
3. Fry, M., and D. E. Green. 1981. Cardiolipin requirement for electron transfer in complex I and III of the mitochondrial respiratory chain. *J. Biol. Chem.* **256:** 1874–1880.
4. Eble, K. S., W. B. Coleman, R. R. Hantgan, and C. C. Cunningham. 1990. Tightly associated cardiolipin in the bovine heart mitochondrial ATP synthase as analyzed by 31P nuclear magnetic resonance spectroscopy. *J. Biol. Chem.* **265:** 19434–19440.
5. Ban, T., J. A. Heymann, Z. Song, J. E. Hinshaw, and D. C. Chan. 2010. OPA1 disease alleles causing dominant optic atrophy have defects in cardiolipin-stimulated GTP hydrolysis and membrane tubulation. *Hum. Mol. Genet.* **19:** 2113–2122.
6. Montessuit, S., S. P. Somasekharan, O. Terrones, S. Lucken-Ardjomande, S. Herzig, R. Schwarzenbacher, D. J. Manstein, E. Bossy-Wetzel, G. Basanez, P. Meda, et al. 2010. Membrane remodeling induced by the dynamin-related protein Drp1 stimulates Bax oligomerization. *Cell.* **142:** 889–901.
7. Gonzalvez, F., Z. T. Schug, R. H. Houtkooper, E. D. MacKenzie, D. G. Brooks, R. J. Wanders, P. X. Petit, F. M. Vaz, and E. Gottlieb. 2008. Cardiolipin provides an essential activating platform for caspase-8 on mitochondria. *J. Cell Biol.* **183:** 681–696.
8. Schlame, M., J. A. Towbin, P. M. Heerdt, R. Jehle, S. DiMauro, and T. J. Blanck. 2002. Deficiency of tetralinoleoyl-cardiolipin in Barth syndrome. *Ann. Neurol.* **51:** 634–637.

9. Hostetler, K. Y., J. M. Galesloot, P. Boer, and H. Van Den Bosch. 1975. Further studies on the formation of cardiolipin and phosphatidylglycerol in rat liver mitochondria. Effect of divalent cations and the fatty acid composition of CDP-diglyceride. *Biochim. Biophys. Acta.* **380:** 382–389.
10. Schlame, M., D. Acehan, B. Berno, Y. Xu, S. Valvo, M. Ren, D. L. Stokes, and R. M. Epand. 2012. The physical state of lipid substrates provides transacylation specificity for tafazzin. *Nat. Chem. Biol.* **8:** 862–869.
11. Taylor, W. A., and G. M. Hatch. 2009. Identification of the human mitochondrial linoleoyl-coenzyme A monolysocardiolipin acyltransferase (MLCL AT-1). *J. Biol. Chem.* **284:** 30360–30371.
12. Cao, J., Y. Liu, J. Lockwood, P. Burn, and Y. Shi. 2004. A novel cardiolipin-remodeling pathway revealed by a gene encoding an endoplasmic reticulum-associated Acyl-CoA:lysocardiolipin acyltransferase (ALCAT1) in mouse. *J. Biol. Chem.* **279:** 31727–31734.
13. Vreken, P., F. Valianpour, L. G. Nijtmans, L. A. Grivell, B. Plecko, R. J. Wanders, and P. G. Barth. 2000. Defective remodeling of cardiolipin and phosphatidylglycerol in Barth syndrome. *Biochem. Biophys. Res. Commun.* **279:** 378–382.
14. Li, H. H., M. S. Willis, P. Lockyer, N. Miller, H. McDonough, D. J. Glass, and C. Patterson. 2007. Atrogin-1 inhibits Akt-dependent cardiac hypertrophy in mice via ubiquitin-dependent coactivation of Forkhead proteins. *J. Clin. Invest.* **117:** 3211–3223.
15. Anderson, E. J., K. A. Thayne, M. Harris, S. R. Shaikh, T. M. Darden, D. S. Lark, J. M. Williams, W. R. Chitwood, A. P. Kypson, and E. Rodriguez. 2014. Do fish oil omega-3 fatty acids enhance antioxidant capacity and mitochondrial fatty acid oxidation in human atrial myocardium via PPARgamma activation? *Antioxid. Redox Signal.* **21:** 1156–1163.
16. Vaden, D. L., V. M. Gohil, Z. Gu, and M. L. Greenberg. 2005. Separation of yeast phospholipids using one-dimensional thin-layer chromatography. *Anal. Biochem.* **338:** 162–164.
17. Ames, B. N., and D. T. Dubin. 1960. The role of polyamines in the neutralization of bacteriophage deoxyribonucleic acid. *J. Biol. Chem.* **235:** 769–775.
18. Bligh, E. G., and W. J. Dyer. 1959. A rapid method of total lipid extraction and purification. *Can. J. Biochem. Physiol.* **37:** 911–917.
19. Fujino, T., M-J. Kang, H. Suzuki, H. Iijima, and T. Yamamoto. 1996. Molecular characterization and expression of rat acyl-CoA synthetase 3. *J. Biol. Chem.* **271:** 16748–16752.
20. Rimessi, A., C. Giorgi, P. Pinton, and R. Rizzuto. 2008. The versatility of mitochondrial calcium signals: from stimulation of cell metabolism to induction of cell death. *Biochim. Biophys. Acta.* **1777:** 808–816.
21. Sprecher, H., D. L. Luthria, B. S. Mohammed, and S. P. Baykousheva. 1995. Reevaluation of the pathways for the biosynthesis of polyunsaturated fatty acids. *J. Lipid Res.* **36:** 2471–2477.
22. Shindou, H., D. Hishikawa, T. Harayama, M. Eto, and T. Shimizu. 2013. Generation of membrane diversity by lysophospholipid acyltransferases. *J. Biochem.* **154:** 21–28.
23. Li, L. O., J. M. Ellis, H. A. Paich, S. Wang, N. Gong, G. Altshuller, R. J. Thresher, T. R. Koves, S. M. Watkins, D. M. Muoio, et al. 2009. Liver-specific loss of long chain acyl-CoA synthetase-1 decreases triacylglycerol synthesis and beta-oxidation and alters phospholipid fatty acid composition. *J. Biol. Chem.* **284:** 27816–27826.
24. Richter-Dennerlein, R., A. Korwitz, M. Haag, T. Tatsuta, S. Dargazanli, M. Baker, T. Decker, T. Lamkemeyer, E. I. Rugarli, and T. Langer. 2014. DNAJC19, a mitochondrial cochaperone associated with cardiomyopathy, forms a complex with prohibitins to regulate cardiolipin remodeling. *Cell Metab.* **20:** 158–171.
25. Baile, M. G., M. Sathappa, Y. W. Lu, E. Pryce, K. Whited, J. M. McCaffery, X. Han, N. N. Alder, and S. M. Claypool. 2014. Unremodeled and remodeled cardiolipin are functionally indistinguishable in yeast. *J. Biol. Chem.* **289:** 1768–1778.
26. Ye, C., W. Lou, Y. Li, I. A. Chatzispyrou, M. Huttemann, I. Lee, R. H. Houtkooper, F. M. Vaz, S. Chen, and M. L. Greenberg. 2014. Deletion of the cardiolipin-specific phospholipase Cld1 rescues growth and life span defects in the tafazzin mutant: implications for Barth syndrome. *J. Biol. Chem.* **289:** 3114–3125.
27. Mulligan, C. M., G. C. Sparagna, C. H. Le, A. B. De Mooy, M. A. Routh, M. G. Holmes, D. L. Hickson-Bick, S. Zarini, R. C. Murphy, F. Y. Xu, et al. 2012. Dietary linoleate preserves cardiolipin and attenuates mitochondrial dysfunction in the failing rat heart. *Cardiovasc. Res.* **94:** 460–468.
28. Ye, C., Z. Shen, and M. L. Greenberg. 2015. Cardiolipin remodeling: a regulatory hub for modulating cardiolipin metabolism and function. *J. Bioenerg. Biomembr.* In press.
29. Houtkooper, R. H., H. Akbari, H. van Lenthe, W. Kulik, R. J. Wanders, M. Frentzen, and F. M. Vaz. 2006. Identification and characterization of human cardiolipin synthase. *FEBS Lett.* **580:** 3059–3064.
30. Zhao, Y., Y. Q. Chen, S. Li, R. J. Konrad, and G. Cao. 2009. The microsomal cardiolipin remodeling enzyme acyl-CoA lysocardiolipin acyltransferase is an acyltransferase of multiple anionic lysophospholipids. *J. Lipid Res.* **50:** 945–956.
31. Schisler, J. C., T. J. Grevengoed, F. Pascual, D. E. Cooper, J. M. Ellis, D. S. Paul, M. S. Willis, C. Patterson, W. Jia, and R. A. Coleman. 2015. Cardiac energy dependence on glucose increases metabolites related to glutathione and activates metabolic genes controlled by mechanistic target of rapamycin. *J. Am. Heart Assoc.* **215:** 4.
32. De, K., G. Ghosh, M. Datta, A. Konar, J. Bandyopadhyay, D. Bandyopadhyay, S. Bhattacharya, and A. Bandyopadhyay. 2004. Analysis of differentially expressed genes in hyperthyroid-induced hypertrophied heart by cDNA microarray. *J. Endocrinol.* **182:** 303–314.
33. Paradies, G., F. M. Ruggiero, G. Petrosillo, and E. Quagliariello. 1994. Enhanced cytochrome oxidase activity and modification of lipids in heart mitochondria from hyperthyroid rats. *Biochim. Biophys. Acta.* **1225:** 165–170.
34. Saini-Chohan, H. K., M. G. Holmes, A. J. Chicco, W. A. Taylor, R. L. Moore, S. A. McCune, D. L. Hickson-Bick, G. M. Hatch, and G. C. Sparagna. 2009. Cardiolipin biosynthesis and remodeling enzymes are altered during development of heart failure. *J. Lipid Res.* **50:** 1600–1608.
35. Sparagna, G. C., C. A. Johnson, S. A. McCune, R. L. Moore, and R. C. Murphy. 2005. Quantitation of cardiolipin molecular species in spontaneously hypertensive heart failure rats using electrospray ionization mass spectrometry. *J. Lipid Res.* **46:** 1196–1204.
36. Iijima, H., T. Fujino, H. Minekura, H. Suzuki, M. J. Kang, and T. Yamamoto. 1996. Biochemical studies of two rat acyl-CoA synthetases, ACS1 and ACS2. *Eur. J. Biochem.* **242:** 186–190.
37. Frahm, J. L., L. O. Li, T. J. Grevengoed, and R. A. Coleman. 2011. Phosphorylation and acetylation of acyl-CoA synthetase- I. *J. Proteomics Bioinform.* **4:** 129–137.
38. Li, L. O., T. J. Grevengoed, D. S. Paul, O. Ilkayeva, T. R. Koves, F. Pascual, C. B. Newgard, D. M. Muoio, and R. A. Coleman. 2015. Compartmentalized acyl-CoA metabolism in skeletal muscle regulates systemic glucose homeostasis. *Diabetes.* **64:** 23–35.
39. Mashek, D. G., L. O. Li, and R. A. Coleman. 2006. Rat long-chain acyl-CoA synthetase mRNA, protein, and activity vary in tissue distribution and in response to diet. *J. Lipid Res.* **47:** 2004–2010.
40. Kiebish, M. A., X. Han, H. Cheng, J. H. Chuang, and T. N. Seyfried. 2008. Cardiolipin and electron transport chain abnormalities in mouse brain tumor mitochondria: lipidomic evidence supporting the Warburg theory of cancer. *J. Lipid Res.* **49:** 2545–2556.
41. Acehan, D., F. Vaz, R. H. Houtkooper, J. James, V. Moore, C. Tokunaga, W. Kulik, J. Wansapura, M. J. Toth, A. Strauss, et al. 2011. Cardiac and skeletal muscle defects in a mouse model of human Barth syndrome. *J. Biol. Chem.* **286:** 899–908.
42. Phoon, C. K., D. Acehan, M. Schlame, D. L. Stokes, I. Edelman-Novemsky, D. Yu, Y. Xu, N. Viswanathan, and M. Ren. 2012. Tafazzin knockdown in mice leads to a developmental cardiomyopathy with early diastolic dysfunction preceding myocardial noncompaction. *J. Am. Heart Assoc.* **1:** pii: jah3-e000455.
43. Barth, P. G., H. R. Scholte, J. A. Berden, J. M. van der Klei-van Moorsel, I. E. M. Luyt-Houwen, E. T. van 'T Veer-Korthof, J. J. van der Harten, and M. A. Sobotka-Plojhar. 1983. An X-linked mitochondrial disease affecting cardiac muscle, skeletal muscle and neutrophil leucocytes. *J. Neurol. Sci.* **62:** 327–355.